ISSN: 2277-3754
ISO 9001:2008 Certified
International Journal of Engineering and Innovative Technology (IJEIT)
Volume 4, Issue 8, February 2015

An analysis on the inserts for piezoelectric bone surgery: the effect of cutting and sterilization processes

De Santis R.[1], Gloria A.[1,*], Russo T.[1], D'Amora U.[1], Lopes Rodrigues D.F.[1], Colella F.[2], Ronca D.[3], Ambrosio L.[1]

[1]Institute of Polymers, Composites and Biomaterials - National Research Council of Italy, V. le J.F. Kennedy 54, Mostra d'Oltremare (Pad.20), 80125, Naples, Italy

[2] Department of Chemical, Materials and Industrial Production Engineering - University of Naples "Federico II", P.le V. Tecchio 80, 80125, Naples, Italy

[3] Institute of Orthopaedics and Traumatology - II University of Naples, Via L. De Crecchio, 2-4, 80138, Naples, Italy

[*]Corresponding author: angloria@unina.it

Abstract*— Piezoelectric bone surgery, also known as piezosurgery, is a technique which has been developed to overcome problems related to conventional surgery through rotating tools such as reamers and drills. Piezosurgery provides a cutting capability of mineralized tissues, however preventing soft tissue damage. Furthermore, it seems that piezosurgery also favors wound healing. Such technique is based on cutting tools (i.e., inserts) vibrating at ultrasonic frequencies. The tip of these inserts is generally covered by a diamond or titanium nitride deposition to enhance the tip hardness, thus improving cutting capability and avoiding instability due to wear. It is well known that efficiency of conventional rotating reamers and drills for bone surgery depends on wear. Anyway, little is known about the coating stability of piezoelectric inserts. Accordingly, the aim of the current work was to analyze the effect of cutting and sterilization processes on the properties of inserts for piezoelectric bone surgery. In particular, the degradation of titanium nitride coating as consequence of a repetitive and controlled 5-cycle cutting/sterilization was studied. SEM and AFM were used to analyze the morphology of the worn coating, while EDS analysis was performed to assess the chemical composition and the element distribution. Results suggested that the stability of titanium nitride coating depends on the quality of the insert. Basically, a poor quality coating negatively affects the cutting process also producing a marked wear of titanium nitride deposition. Bulk alloy was exposed, mainly consisting of iron, as well as alloying elements and impurities (i.e., manganese and sulfur) which may be dangerous for the health of the patient.

***Index Terms*— piezosurgery, inserts, cutting/sterilization process, EDS, morphological features.**

I. INTRODUCTION

Piezoelectric bone surgery, also known as piezosurgery, is an advanced technique for cutting mineralized tissues. (1) The process relies on the piezoelectric effect, discovered in 1880 by the Curie brothers (2), through which an electric field is directly converted by a piezo-ceramic crystal into mechanical strain. This technique has been showed to be particularly suitable to finely grind brittle and semi-brittle materials such as ceramics. (3) The extracellular matrix of hard tissue (i.e. bone and dentin) mainly consists of collagen and hydroxyapatite. Mechanical properties of these tissues largely depend on the porosity, however bone and dentin are considered semibrittle materials. (4-7) In 1988 ultrasonic techniques were implemented in surgery for cutting mineralized tissue. (8) Tool tips, known as inserts, allow to transfer the mechanical strain to biological tissues providing a cutting capability that occurs exclusively on hard tissue. (9)

This technique has been proved to be effective in many fields of the maxillofacial surgery (10,11), but also the orthopaedic surgery has benefit from this technique. (12) Compared to other conventional bone cutting techniques involving rotating instruments, piezosurgery has shown to favor wound healing. (13,14) Moreover, it is reported that piezoelectric surgery is less harmful than conventional rotating tools for the nerve. (15) Thus, piezosurgery represents a promising tool for performing bone surgery involving districts close to nerves.

Several inserts of different shape and size, such as flat scalpel, cone compressor, sharp-tipped saw and bone harvester, have been developed for specific surgery applications. (11) The cutting insert tip is generally coated with diamond or titanium nitride to improve cutting capability and to avoid the insert stability due to wear. (1) These inserts are driven by a piezoelectric crystal oscillating at a frequency selectable between 25 and 30 kHz. The highest frequency, known as boosted modality, is generally adopted for bone surgery. To prevent overheating, a water jet cools the vibrating elements. The micro vibration amplitude of inserts is estimated to be between 60 and 210 µm. (1)

As reported the cutting efficiency and quality of conventional rotating reamers and drills for bone surgery depend on the wear of rotating tools. (16,17) Thus, hard coatings are generally implemented on the blades of these rotating tools, especially when precise cuttings and insert stability are required. (18,19) The performance of TiN coatings on these conventional tools is well documented. (20)

ISSN: 2277-3754
ISO 9001:2008 Certified
International Journal of Engineering and Innovative Technology (IJEIT)
Volume 4, Issue 8, February 2015

Another important source data concerning wear of TiN coatings is represented by end prostheses and joint prostheses in dentistry and orthopedics. (21,22)

On the other hand, the topography and quality of TiN coatings depend on the deposition process and process parameters. Different topographies can be distinguished at micro and nano scale levels according to the deposition processing conditions. (23,24) Clearly, different wear patterns and quality and/or stability of coatings have been observed. (23,25)

To the authors' knowledge, little is known regarding wear/degradation and stability of titanium nitride (TiN) deposition on piezoelectric inserts and on the effect of wear on the cutting precision and quality. Accordingly, the aim of the current research was to evaluate the effect of cutting and sterilization processes on the properties of inserts for piezoelectric bone surgery. Specifically, the degradation of titanium nitride coating as consequence of a repetitive and controlled 5-cycle cutting/sterilization was studied. SEM and AFM were used to analyze the morphology of the worn coating, while EDS analysis was performed to assess the chemical composition and the element distribution.

II. MATERIALS AND METHODS

The Mectron PIEZOSURGERY 3® equipment (Mectron SpA, Carasco, Genova, Italy) was used in conjunction with different inserts such as OP3 bone scalpel and OT7 sharp tipped saw, which are suitable for osteoplasty and osteotomy, respectively. Two samples of OP3 inserts, namely Sample A-OP3 produced by Mectron SpA, and Sample B-OP3 produced by Asian industry, were used. Furthermore, two samples of OT7 inserts, namely Sample A-OT7 produced by Mectron SpA, (Carasco, Genova, Italy) and Sample B-OT7 produced by Asian industry, were also employed.

Glass fiber reinforced polyetherimide (GF/PEI) plates were used as cortical bone analogue materials. Such composite has the same stiffness of the cortical bone. (26-29) Polyurethane (PU) plates (Type ERP #1522-03), which have properties similar to bone (30,31), were purchased from Sawbones® (Malmo, Sweden).

A. Controlled bone analogue cutting process

To investigate the effect of cutting on wear of piezoelectric inserts an automated cutting process was developed. The experimental set-up, shown in fig. 1, consisted in a modified 3D bioplotter system. (32-34) Briefly, a three stage system consisting in three mechanical linear guides, driven by stepper motors, allowed a fine control (positioning precision of 1 µm) for the X,Y,Z movement. A polymeric container was fixed on the X,Y stages. This container allowed collecting cooling water of the piezosurgery equipment. The PU or the composite GF/PEI plates were fixed inside the container. The piezoelectric hand piece was fixed to the z stage through a cylindrical hinge (fig. 1b). The z stage was positioned to obtain an angle of 90° between the composite plate and the cutting insert tip. OT7 and OP3 inserts were used to cut PU and GF/PEI, respectively. To standardize the pressure acting on the inserts, hollow stainless cylinders, with a weight of 200 g or 600 g, were applied on the piezoelectric handpiece in order to cut spongy and cortical bone analogue materials through the OT7 and OP3 inserts, respectively (fig. 1b and 1c).

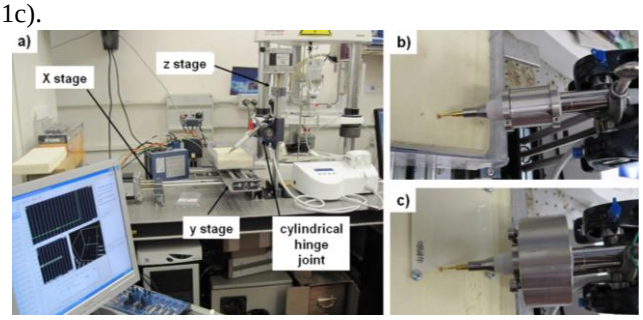

Fig. 1. Experimental set-up to perform controlled cutting of bone analogue materials through the piezosurgery equipment: 1a) modified 3D bioplotter system comprising a cylindrical hinge to fix the piezoelectric hand piece; 1b) hand piece equipped with a 200 g weight to cut spongy bone analogue materials (PU plates); 1c) hand piece equipped with a 600 g weight to cut cortical bone analogue materials (GF/PEI plates).

The 3D Bioplotter system was controlled by a LabView software (National Instruments, Assago, Milano, Italy). The cutting speed was set at 3.5 cm/min and 7 cm/min, for spongy and cortical bone, respectively. Each job consisted of 5 consecutive and linear cuttings, each covering a distance of 15 cm. Each job included three resting periods of 20 min to prevent overheating and the autoclave sterilization process at 120°C in the final stage of the wearing job. Each insert underwent through 5 consecutive jobs.

B. Microscopy Investigations

Scanning electron microscopy (SEM) using the FEI Quanta FEG 200 apparatus (The Netherlands) was performed on all the samples to detect the morphology of the different cutting insert tip. Moreover, SEM imaging was also performed on inserts which underwent five cycles of wear due to cutting through the modified 3D bioplotter system and 5 cycles of sterilization in autoclave at 120°C.

Atomic Force Microscopy (AFM) was performed on Sample A-OP3 and Sample B-OP3 using the AFM Perception equipment (Assing, Italy) to assess the surface roughness of the cutting tip of the inserts. 20 areas (19 x 19 μm^2) for each sample were analyzed in contact mode, and bidimensional images (500 × 500 lines) were elaborated through the Gwyddion software to measure the mean roughness (R_a) and the root mean square (RMS) roughness (R_q).

C. Energy Dispersive X-Ray Spectrometry (EDS)

Energy Dispersive X-ray Spectrometry (EDS) was performed on the cutting tip of each insert to analyze the surface material composition. The FEI Quanta FEG 200 equipment (The Netherlands) was used. Elemental distribution maps of N, Ti, Fe, and Cr elements were implemented to analyze the quality of the insert coating.

ISSN: 2277-3754
ISO 9001:2008 Certified
International Journal of Engineering and Innovative Technology (IJEIT)
Volume 4, Issue 8, February 2015

EDS was also performed on inserts which underwent to five cycles of wear due to cutting and 5 cycles of sterilization in autoclave at 120°.

III. RESULTS

Well defined and precise tracks were observed on the composite plates (i.e., cortical bone analogue materials) which underwent cutting through Sample A-OP3 insert. In particular, deeper and rougher tracks were observed on the composite plates which underwent cutting through Sample A-OP3 insert.

Fig. 2 shows SEM images of Sample A-OT7 inserts before (fig. 2a, 2b and 2c) and after (fig. 2d, 2e and 2f) the 5-cycle cutting/sterilization process. Macro-details of the sharp tipped saw, suitable for osteotomy, can be detected in fig. 2a, while micro-details of the surface before the 5-cycle cutting/sterilization process, showing a smooth homogeneous topography, can be detected in fig. 2b and 2c. After the 5-cycle cutting/sterilization process evident wear of the cutting surfaces characterized by stripes (fig. 2d and 2e) and pits (fig. 2f) can be clearly observed.

Fig. 3 shows SEM images of Sample B-OT7 inserts before (fig. 3a, 3b and 3c) and after (fig. 3d, 3e and 3f) the 5-cycle cutting/sterilization process. Macro-details of the sharp tipped saw, suitable for osteotomy, can be detected in fig. 3a, while micro-details of the surface before the cutting/sterilization process, showing a smooth homogeneous topography, can be detected in fig. 3b and 3c. After the 5-cycle cutting/sterilization process wear was evident on the surfaces (fig. 3d). Furthermore, the morphology of deep pits was detected at higher magnification (fig. 3e and 3f).

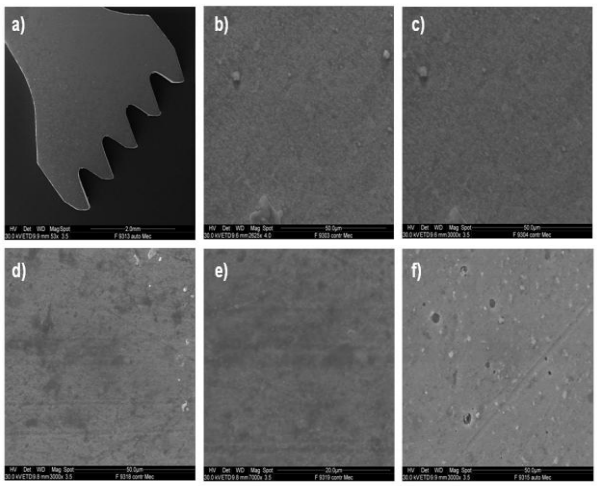

Fig. 2. Results from SEM on Sample A-OT7 insert before (a, b and c) and after (d, e and f) the 5-cycle cutting/sterilization processes. Macro-details of the sharp tipped saw is shown in figure a); micro-details of the surface before the cutting/sterilization process are shown in fig. b and c. Evident wear due to the 5-cycle cutting/sterilization processes of the cutting surfaces characterized by stripes can be detected in d) and e), while evident pits can be observed in f).

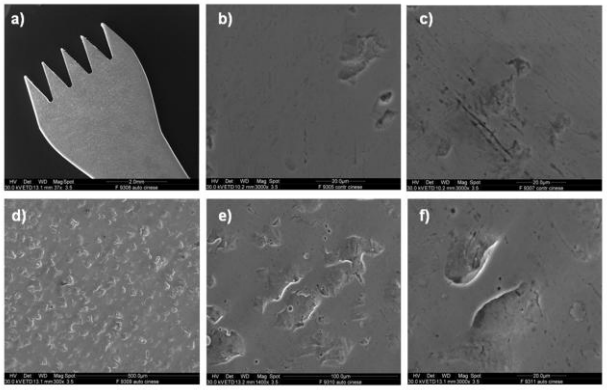

Fig. 3. Results from Sample B-OT7 insert before (a, b and c) and after (d, e and f) the 5-cycle cutting/sterilization process. Macro-details of the sharp tipped saw is shown in fig. a); micro-details of the surface before the cutting/sterilization process are shown in fig. b and c. Evident wear characterized by pits diffused all over the cutting surface are shown in d, depth of these pits can be detected in fig. e) and f).

AFM topographic images (19×19 μm^2 area) of Sample A-OP3 (fig. 4a and 4b) and Sample B-OP3 (fig. 4c and 4d) are reported. Both Samples A-OP3 and B-OP3 have shown an assembly of rhomboidal dots, even if a densely packed assembly can be observed for Samples A-OP3, while a less dense one can be detected for Sample B-OP3.

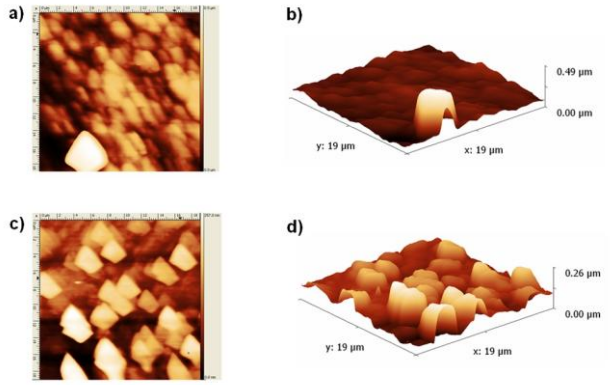

Fig. 4. Results from AFM analysis: surface topography detected on a 19×19μm^2 area. a) 2D imaging of Samples A-OP3; b) 3D imaging of Samples A-OP3; c) 2D imaging of Samples B-OP3; d) 3D imaging of Samples B-OP3.

Mean roughness (R_a) of 30.7 ± 6.9 nm and root mean square roughness (R_q) of 45.8 ± 12.8 nm have been obtained for Samples A-OP3 by averaging 20 scans on 19×19 μm^2 areas, whilst for Samples B-OP3 roughness values of 24.9 ± 12.1 nm and 38.4 ± 18.8 nm have been evaluated in terms of R_a and R_q, respectively.

SEM images of bone scalpel inserts, Samples A-OP3 and B-OP3, are reported in fig. 5a and 5c, respectively. EDS on Samples A-OP3 and B-OP3 are shown in fig. 5b and 5d, respectively. A consistent deposition of titanium nitride (TiN) can be observed on the cutting tip of Samples A-OP3 insert (fig. 5a), while a mild TiN deposition can be observed on the cutting tip of Samples B-OP3 insert (fig. 5c). Morphology detected by SEM of these samples is consistent with

ISSN: 2277-3754
ISO 9001:2008 Certified
International Journal of Engineering and Innovative Technology (IJEIT)
Volume 4, Issue 8, February 2015

topography detected by AFM (fig. 4). The distribution of titanium (red channel) and iron (green channel) of Samples A-OP3 and of Samples B-OP3 is shown in fig. 5b and 5c, respectively. A homogeneous distribution of titanium, almost covering all the cutting tip of the scalpel insert can be appreciated for Samples A-OP3 (fig. 5b), and abundant trace of titanium can also be detected far from the cutting tip of this insert. A moderate titanium deposition has been observed for sample B-OP3, and such deposition seems to be absent from the cutting tip where iron mainly prevails.

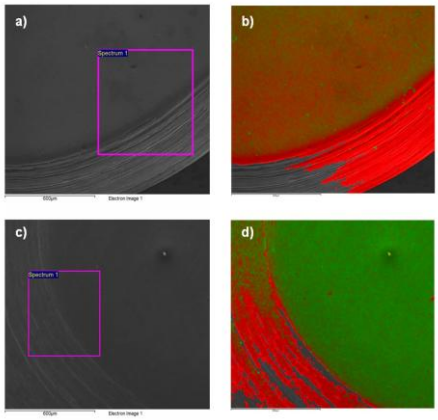

Fig. 5. Results from SEM and EDS analysis on bone scalpel inserts. a) SEM images of Samples A-OP3 showing the morphology of the cutting tip and the spectrum region into which EDS was performed; b) distribution of titanium (red channel of the map) and iron (green channel) for Samples A-OP3; c) SEM imaging of Samples B-OP3 showing the morphology of the cutting tip and the spectrum region into which EDS was performed; d) distribution of titanium (red channel) and iron (green channel) for Samples B-OP3.

Fig. 6 reports the element analysis for Samples A-OP3 and B-OP3 corresponding to the regions detected by the pink rectangles (fig. 5a) and 5c), respectively). The amount of titanium on Samples A-OP3 is about fourfold that of samples B-OP3. Of course, a much higher content of iron has been evaluated for Samples B-OP3. Surprisingly, manganese traces have been also detected and quantified for Samples B-OP3 (fig. 6b).

a)

Element	Weight%	Atomic%
N K	23.18	51.93
Ti K	51.16	33.51
Cr K	3.30	1.99
Fe K	22.36	12.56
Totals	100.00	

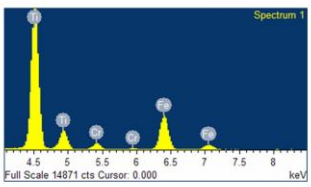

b)

Element	Weight%	Atomic%
N K	10.51	31.25
Ti K	11.38	9.89
Cr K	11.23	8.99
Mn K	0.88	0.67
Fe K	66.00	49.20
Totals	100.00	

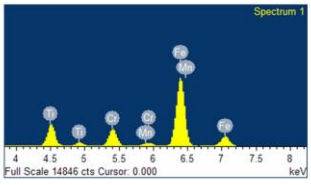

Fig. 6. Results from EDS analysis on Samples A-OP3 and B-OP3 performed in the regions detected by the pink rectangles in fig. 5a) and 5c), respectively. a) Distribution of elements for Samples A-OP3; b) distribution of elements for Samples B-OP3.

Fig. 7 shows SEM and EDS imaging for Samples A-OT7 and B-OT7 after the 5-cycle cutting/sterilization process. SEM morphology of Samples A-OT7 and B-OT7 are presented in fig. 7a) and 7e), respectively. The pink rectangles reported into these images detect the region into which EDS was performed to quantify element analysis and distribution. Fig. 7b), 7c) and 7d) show the EDS maps concerning nitrogen, iron and titanium distribution, respectively, for Samples A-OT7. Fig. 7f), 7g) and 7h) show nitrogen, iron-titanium (channels green and red, respectively) and manganese distribution for Samples B-OT7.

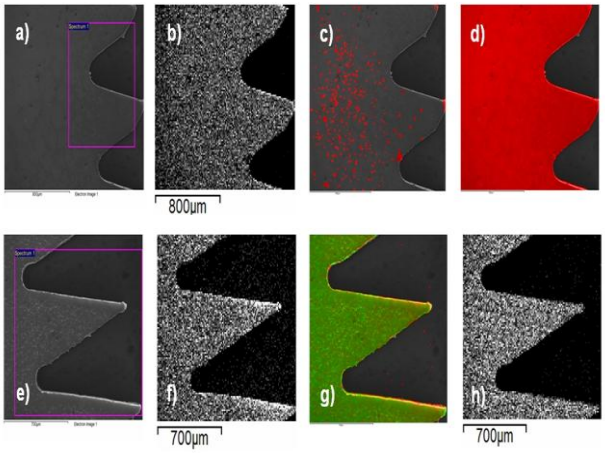

Fig. 7. Results from SEM and EDS analysis on Samples A-OT7 and B-OT7 after 5-cycle cutting/sterilization process. a) SEM morphology of Samples A-OT7, the pink rectangles detects the region into which X-ray spectroscopy for element quantification and distribution was performed; b) nitrogen map for Sample A-OT7; c) iron map for Sample A-OT7; d) titanium map for Sample A-OT7; e) SEM images of Sample B-OT7, the reported pink rectangles highlight the region into which EDS for element quantification was performed; f) nitrogen map for Sample B-OT7; g) iron-titanium maps (channels - green and red, respectively) for Sample B-OT7; h) manganese map for Sample B-OT7.

Fig. 7d) clearly shows that a homogeneous distribution of titanium completely covers almost of the surface of Sample A-OT7 even after the 5-cycle cutting/sterilization process. On the other hand, fig. 7g) suggests a lack of titanium on Sample B-OT7 after wearing due to the 5-cycle cutting/sterilization processes. The alloy based on iron and manganese composing the bulk Sample B-OT7 is clearly evident in fig. 7g) and 7h).

Table 1 reports the elemental distribution from EDS analysis on Samples A-OT7 and B-OT7 after the 5-cycle cutting/sterilization process, performed in the regions highlighted by the pink rectangles of fig. 7a) and 7g). The amount of titanium on Samples A-OT7 is about one-fold higher than that of Samples B-OT7. Consequently, a much higher content of iron is measured for Samples B-OT7. Furthermore, traces of elements such as manganese and sulfur have also been detected and quantified for Samples B-OT7.

ISSN: 2277-3754
ISO 9001:2008 Certified
International Journal of Engineering and Innovative Technology (IJEIT)
Volume 4, Issue 8, February 2015

Table 1. Elemental distribution for samples OT7 after the 5-cycle cutting/sterilization process detected in the regions delimitated by the pink rectangles in figures 7a) and 7e).

	Sample A-OT7		Sample B-OT7	
Element	Weight %	Atomic %	Weight %	Atomic%
N-K	22.11	49.50	1.49	3.45
Ti-K	72.41	47.39	7.96	8.85
Cr-K	0.98	0.59	13.38	13.71
Fe-K	4.50	2.52	75.90	72.38
S-K	-	-	0.55	0.91
Mn-K	-	-	0.72	0.69
Total	100		100	

IV. DISCUSSION

Even if engineered polymers and composites can be suitably tailored to match mechanical properties of mineralized tissues (4,5,7), wear strongly depends on friction between cutting tool and material. (19,23,24) As friction is related to both surface chemistry and topography, materials which loosely resemble the features of natural tissues negatively affect the friction process. However, compared to single phase materials, reinforced polymers are considered a suitable class of materials for cutting processes. (20)

Anyway, it is very difficult to standardize a wear process of cutting inserts on natural hard tissues for several reasons. Specifically, the amount of constituents and the morphological/architectural features of natural tissues are common constraints. Moreover, the properties of hard tissues depend on the anatomical district, in particular physical/chemical properties widely change among tissues even if they are collected from the same district. (4) Therefore, to standardize the cutting process through piezosurgery, the use of synthetic polymers and composites as bone analogue materials represents the only rational solution. Furthermore, the use of a modified injection/extrusion-based system (i.e., 3D Bioplotter/Bioextruder) (32-37) allowed to finely control relative movements between the piezoelectric inserts and analogue polymer-based substrates.

The SEM morphology of untreated inserts of Samples A and B (fig. 2b, 2c and 3b, 3c, respectively) clearly showed a difference that can be ascribed to the coating process. Defects such as voids, pits and tracks can be easily observed on the coating of Sample B inserts. However, a rougher topography after cycling is observed for both samples. Bigger voids, marked tracks and higher number of pits are observed (fig. 3d, 3e, 3f and 4d, 4e, 4f). These morphologies and defects due to wear are similar to those detected on prosthetic coatings and conventional cutting tools. (21-23)

AFM analysis revealed a complex topography of the coating composed by grains of different size (fig. 4). A smooth polycrystalline surface made of grains with dimension lower than 1µm can be observed, while bigger grains with a dimension of 4 µm have been detected in the regions close to the cutting tip of the inserts. Bigger size grains of TiN coatings are generally obtained through greater deposition energy involving higher ion flux, and they result in the conglomeration of smaller size grains. (19)

Consistently with SEM and AFM results, EDS mapping also revealed a thick and homogeneous TiN coating completely covering the surface tip of Sample A inserts (fig. 5b). Chemical composition of Sample A coating (fig. 6a) clearly indicates a high amount of Ti(Kα), positioned at about 4.5 keV, and a lower amount of Ti(Kβ), positioned at about 4.9 keV. The ratio of Ti(Kα)/ Ti(Kβ) is similar for both samples, and these results are consistent with titanium nitride coatings on hip implants. (21)

Nevertheless, significant chemical differences have been detected between Samples A and B (fig. 6 and table 1). The difference in terms of Ti-K/N-K between Samples A and B suggests that the process adopted for coating Sample B also involves deposition of chromium nitride. Although it has been reported that chromium nitride may provide enhanced corrosion and wear resistances, (25) sample B clearly showed a marked degradation of the coating in terms of topography and composition (fig. 7g and table 1). Moreover, the high Fe-K amount on Sample B inserts, as well as Mn-K trace, suggest that sample B coating does not completely cover the tip of the insert. (19) Alloy impurities, such as sulfur, are also detected after the cycling process for Sample B (Table 1). The relative variation of the Ti-K peak intensity of the coating with respect to Fe-K ones of the bulk alloy is due to the different thicknesses of films. It has been suggested that the Ti-K/Fe-K peak intensity ratio provides an estimation of the average thickness of the deposited TiN. (19)

The higher cutting precision of Sample A may be probably related to the superior quality of the developed TiN coating as evidenced by SEM, AFM and EDS analyses on these inserts.

V. CONCLUSION

Results suggested that the stability of titanium nitride deposition covering the tip depends on the quality of the insert. In particular, a poor quality coating negatively affects the cutting process, also producing a marked wear of titanium nitride deposition of the titanium nitride deposition. With regard to Sample B, bulk alloy was exposed, mainly consisting of iron, as well as alloying elements and impurities (i.e., manganese and sulfur) which may be dangerous for the health of the patient. The current research represents a first step towards an innovative process in the biomedical field aiming to combine piezosurgery with the more advanced CAD/CAM techniques.

ACKNOWLEDGMENT

The authors thank Dr. Gianluca Ametrano from the University of Naples “Federico II” for his contribution in performing the AFM analysis.

This project has received funding also from the European Union’s Seventh Framework Programme for research,

ISSN: 2277-3754
ISO 9001:2008 Certified
International Journal of Engineering and Innovative Technology (IJEIT)
Volume 4, Issue 8, February 2015

technological development and demonstration under grant agreement number 317304.

REFERENCES

[1] G. Pavlikovà, R. Foltàn, M. Horkà, T. Hanzelka, H. Borunskà and J. Sedy, "Piezosurgery in oral and maxillofacial surgery", Int. J. Oral Maxillofac. Surg., 40, pp. 451–457, 2011.

[2] S. C. Masmanidis, R. B. Karabalin, I. De Vlaminck, G. Borghs, M. R. Freeman and M. L. Roukes, "Multifunctional Nanomechanical Systems via Tunably Coupled Piezoelectric Actuation", Science, Vol. 317 (5839), pp. 780-783, 2007.

[3] K. Mizutani, T. Kawano and Y. Tanaka, "A piezoelectric-drive table and its application to micro-grinding of ceramic materials", Precis. eng., 12 (4) pp. 219-226, 1990.

[4] R. De Santis, L. Ambrosio, F. Mollica, P. Netti and L. Nicolais. "Mechanical properties of human mineralized connective tissues" Modeling of Biological Materials, eds Mollica, F., Preziosi, L. and Rajagopal, K.R, (Birkhauser: Boston), pp. 211-261, 2007.

[5] D. Ronca, A. Gloria, R. De Santis, T. Russo, U. D'Amora, M. Chierchia, L. Nicolais and L. Ambrosio, "Critical analysis on dynamic-mechanical performance of spongy bone: the effect of an acrylic cement", Hard Tissue, 11, 3, pp.1-9, 2014.

[6] R. De Santis, D. Prisco, S. N. Nazhat, F. Riccitiello, L. Ambrosio, S. Rengo and L. Nicolais, "Mechanical strength of tooth fragment reattachment", J. biomed. mater. res., 55 (4), pp. 629-636, 2001.

[7] R. De Santis, A. Gloria, T. Russo, U. D'Amora, A. Varriale, M. Veltri, P. Balleri, F. Mollica, F. Riccitiello and L. Ambrosio, "Reverse engineering of mandible and prosthetic framework: Effect of titanium implants in conjunction with titanium milled full arch bridge prostheses on the biomechanics of the mandible", J. Biomech., 47, pp. 3825–3829, 2014.

[8] T. Vercellotti, S. De Paoli and M. Nevins, "The piezoelectric bony window osteotomy and sinus membrane elevation: introduction of a new technique for simplification of the sinus augmentation procedure", Int. J. Periodontics Restorative Dent., 21(6), pp. 561-67, 2001.

[9] E. Crosetti, B. Battiston and G Succo. "Piezosurgery in head and neck oncological and reconstructive surgery: personal experience on 127 cases", Acta Otorhinolaryngol. Ital., 29, pp. 1-9, 2009.

[10] S.S. Wallace, S.J. Froum, S.C. Cho and D.P. Tarnow, "Schneiderian membrane perforation rate during sinus elevation using piezosurgery: clinical results of 100 consecutive cases", Int. J. Periodontics Restorative Dent., 27, pp. 413-419, 2007.

[11] G. Eggers, J. Klein, J. Blank and S. Hassfeld. "Piezosurgery®: an ultrasound device for cutting bone and its use and limitations in maxillofacial surgery", British J. Oral Maxillofacial Surg. 42, pp. 451-453, 2004.

[12] D. J. Hoigne, S. Stübinger, O. Von Kaenel, S. Shamdasani and P. Hasenboehler, "Piezoelectric osteotomy in hand surgery: first experiences with a new technique", BMC Musculoskelet Disord., 12:, 36, 2006.

[13] T. Vercellotti, M. L. Nevins, D. M. Kim, M. Evins, K. Wada, R. K. Schenk and J. P. Fiorellini, "Osseous response following respective therapy with piezosurgery", Int. J. Periodontics Restorative Dent., 25, pp. 543-549, 2005.

[14] G. Chiriac, M. Herten, F. Schwarz, D. Rothamel and J. Becker "Autogenous bone chips: influence of a new piezoelectric device (Piezosurgery®) on chip morphology, cell viability and differentiation", J. Clin. Periodontol. 32, pp. 994–999, 2005.

[15] S. Schaeren, C. Jaquie´ry, M. Heberer, M. Tolnay, T. Vercellotti and I. Martin, "Assessment of nerve damage using a novel ultrasonic device for bone cutting", J. Oral. Maxillofac. Surg. 66, pp. 593–596, 2008.

[16] C. Ercoli, P. D. Funkenbusch, H. J. Lee, M. E. Moss and G. N. Graser "The influence of drill wear on cutting efficiency and heat production during osteotomy preparation for dental implants: a study of drill durability", Int. J. Oral Maxillofac. Implants, 19, pp. 335–349, 2004.

[17] G. E. Chacon, D. L. Bower, P. E. Larsen, E. A. Mc Glumphy and F. M. Beck, "Heat production by 3 implant drill systems after repeated drilling and sterilization", J. Oral Maxillofac. Surg. 64, pp. 265–269, 2006.

[18] M. Uchid, N. Nihira, A. Mitsuo, K. Toyoda, K. Kubot, T. Aizaw, "Friction and wear properties of CrAlN and CrVN films deposited by cathodic arc ion plating method", Surf. Coatings Technol., 177 (178), pp. 627–630, 2004.

[19] R. S. Rawat, W. M. Chew, P. Lee, T. White and S. Lee, "Deposition of titanium nitride thin films on stainless steel-AISI 304 substrates using a plasma focus device", Surf. Coat. Technol., 173, pp. 276–284, 2003.

[20] G. Murphy Byrne and M. D. Gilchrist, "The performance of coated tungsten carbide drills when machining carbon fibre-reinforced epoxy composite materials", Proc. Inst. Mech. Eng., Part B, 216 (2), pp. 143-152, February 2002.

[21] M. K. Harman, S. A. Banks, and W. A. Hodge, "Wear Analysis of a Retrieved Hip Implant with Titanium Nitride Coating", J. Arthroplasty, 12 (8), pp. 938-945, 1997.

[22] M. T. Raimondi and R. Pietrabissa, "The in-vivo wear performance of prosthetic femoral heads with titanium nitride coating", Biomaterials, 21, pp. 907-913, 2000.

[23] D. Nolan, S.W. Huang, V. Leskovsek and S. Braun, "Sliding wear of titanium nitride thin films deposited on Ti–6Al–4V alloy by PVD and plasma nitriding processes", Surf. Coat. Technol., 200, pp. 5698-5705, 2006.

[24] C. Muratore, J.J. Hu, and A.A. Voevodi, "Adaptive nanocomposite coatings with a titanium nitride diffusion barrier mask for high-temperature tribological applications", Thin Solid Films, 515, pp. 3638-3643, 2007.

[25] M. Uchida, N. Nihira, A. Mitsuo, K. Toyoda, K. Kubota and T. Aizawa, "Friction and wear properties of CrAlN and CrVN films deposited cathodic arc ion plating method", Surf. Coat. Technol., 177 (178), pp. 627–630, 2004.

[26] A. Gloria, D. Ronca, T. Russo, U. D'Amora, M. Chierchia, R. De Santis, L. Nicolais and L. Ambrosio, "Technical features and criteria in designing fiber-reinforced composite materials: from the aerospace and aeronautical field to biomedical applications", J. appl. biomater. biomech., 9 (2), pp. 151-163, 2010.

[27] R. De Santis, F. Sarracino, F. Mollica, P. A. Netti, L. Ambrosio and L. Nicolais, "Continuous fibre reinforced polymers as

ISSN: 2277-3754
ISO 9001:2008 Certified
International Journal of Engineering and Innovative Technology (IJEIT)
Volume 4, Issue 8, February 2015

connective tissue replacement", Compos. sci. technol., 64 (6), pp. 861-871, 2004.

[28] R. De Santis, L. Ambrosio and L. Nicolais, "Polymer-based composite hip prostheses", J. inorg. biochem., 79 (1), pp. 97-102, 2000.

[29] A. Merolli, V. Perrone, P. T. Leali, L. Ambrosio, R. De Santis, L. Nicolais and C. Gabbi, "Response to polyetherimide based composite materials implanted in muscle and in bone", J. Mater. Sci. Mater. Med., 10 (5), pp. 265-268, 1999.

[30] R. De Santis, F. Mollica, R. Esposito, L. Ambrosio and L. Nicolais, "An experimental and theoretical composite model of the human mandible", J. Mater. Sci. Mater. Med., 16 (12), pp. 1191-1197, 2005.

[31] R. De Santis, F. Mollica, F. Zarone, L. Ambrosio and L. Nicolais, "Biomechanical effects of titanium implants with full arch bridge rehabilitation on a synthetic model of the human jaw", Acta biomater., 3 (1), pp. 121-126, 2007.

[32] R. De Santis, A. Gloria, T. Russo, U. D'Amora, S. Zeppetelli, C. Dionigi, A. Sytcheva, T. Herrmannsdorfer, V. Dediu and L. Ambrosio, "A Basic Approach Toward the Development of Nanocomposite Magnetic Scaffolds for Advanced Bone Tissue Engineering", J. Appl. Polym. Sci., 122, pp. 3599–3605, 2011.

[33] A. Gloria, F. Causa, T. Russo, E. Battista, R. Della Moglie, S. Zeppetelli, R. De Santis, P. A. Netti and L. Ambrosio, "Three-dimensional poly (ε-caprolactone) bioactive scaffolds with controlled structural and surface properties", Biomacromolecules, 13(11), pp. 3510-21. 2012.

[34] D. Puppi, C. Mota, M. Gazzarri, D. Dinucci, A. Gloria, M. Myzabekova, L. Ambrosio, and F. Chiellini, "Additive manufacturing of wet-spun polymeric scaffolds for bone tissue engineering", Biomed. Micro devices, 14 (6), pp. 1115-1127, 2012.

[35] R. Santis, A. Gloria, T. Russo, U. D'Amora, V. D'Antò, F. Bollino, M. Catauro, F. Mollica, S. Rengo and L. Ambrosio, "Advanced composites for hard-tissue engineering based on PCL/organic-inorganic hybrid fillers: From the design of 2D substrates to 3D rapid prototyped scaffolds", Polym. Compos., 34 (9), pp. 1413-1417, 2013.

[36] T. Patricio, M Domingos, A. Gloria, U. D'Amora, J. F. Coelho and P. J. Bártolo. "Fabrication and characterisation of PCL and PCL/PLA scaffolds for tissue engineering", Rapid Prototyp. J., 20(2), pp. 145-156, 2014.

[37] R. De Santis, A. Russo, A. Gloria, U. D'Amora, T. Russo, S. Panseri, M. Sandri, A. Tampieri, M. Marcacci, V. A. Dediu, C. J. Wilde and Luigi Ambrosio, "Towards the Design of 3D Fiber-Deposited Poly(ε-caprolactone)/Iron-Doped Hydroxyapatite Nanocomposite Magnetic Scaffolds for Bone Regeneration", J. Biomed. Nanotechnol., 11, pp. 1236-1246, 2015.